



Citation for published version:

Zhou, N, Zhang, Y, Bowen, CR & Cao, J 2020, 'A stacked electromagnetic energy harvester with frequency up-conversion for swing motion', *Applied Physics Letters*, vol. 117, no. 16, 163904.
<https://doi.org/10.1063/5.0025520>

DOI:

[10.1063/5.0025520](https://doi.org/10.1063/5.0025520)

Publication date:

2020

Document Version

Peer reviewed version

[Link to publication](#)

Copyright 2020 AIP Publishing.

Zhou, N, Zhang, Y, Bowen, CR & Cao, J 2020, 'A stacked electromagnetic energy harvester with frequency up-conversion for swing motion', *Applied Physics Letters*, vol. 117, no. 16, 163904.
<https://doi.org/10.1063/5.0025520>

University of Bath

Alternative formats

If you require this document in an alternative format, please contact:
openaccess@bath.ac.uk

General rights

Copyright and moral rights for the publications made accessible in the public portal are retained by the authors and/or other copyright owners and it is a condition of accessing publications that users recognise and abide by the legal requirements associated with these rights.

Take down policy

If you believe that this document breaches copyright please contact us providing details, and we will remove access to the work immediately and investigate your claim.

A stacked electromagnetic energy harvester with frequency up-conversion for swing motion

Ning Zhou¹, Ying Zhang¹, Chris R. Bowen², Junyi Cao^{1,a)}

¹Key Laboratory of Education Ministry for Modern Design and Rotor-Bearing System, School of Mechanical Engineering, Xi'an Jiaotong University, Xi'an 710049, China

²Materials and Structures Centre, Department of Mechanical Engineering, University of Bath, Bath, BA27AY, UK

Abstract

This paper undertakes theoretical and experimental investigations of a stacked magnetic modulation harvester with frequency up-conversion for maximum harvesting of energy from swing motion. The harvester includes stacked rings including coils, an energy harvesting magnetic ring, a ferromagnetic ring, and a frequency up-conversion magnetic ring with proof mass, which are axially designed in the same rotating axis to increase the rotation speed of the magnetic field due to swing excitations from human motion. The magnetic flux density produced by frequency up-conversion mechanisms are calculated to derive the governing theoretical model for harvester performance prediction. The rotation speeds and inductive voltages of theoretical results show good agreement with the experimental results at a range of rotational speeds. A range of motion speeds tests on a treadmill are performed to demonstrate the advantage of the stacked electromagnetic harvesters on harvested energy from human motion. The average output power improves from approximately 1.5mW to 11.8mW when walking speed increases from 4km/h to 8km/h; the maximum power density under human motion is $61.9\mu\text{W}\cdot\text{g}^{-1}$, with total weight of 190.7g.

Keyword: Energy harvesting, Magnetic modulation, Performance enhancement, Limb swing.

^a Author to whom correspondence should be addressed. Electronic mail: caojy@mail.xjtu.edu.cn.

The idea of harvesting energy from human motion to power low-power devices, including wearable devices, has become feasible as a result of recent advances in low-power microelectronics and energy harvesting devices. A variety of structures have been proposed and tested, which are often based on the mechanism of piezoelectric^{1,2}, triboelectric^{3,4}, and electromagnetic^{5,6} effects. For wearable items that range from a backpack⁷ to the boots¹, the mechanical energy contained in a range of human motions have been considered. These include the swing of the upper-limb and lower-limb⁸, the oscillation of the center of mass of a human body⁹, the rotation of joints¹⁰ and walking pressure¹¹, which have all been efficiently utilized in the last decade. Rome *et al.*¹² developed a suspended-load backpack and generated power of 7.4W. Halim *et al.*¹³ designed an electromagnetic rotation energy harvester using a sprung eccentric rotor to generate a power of 61.3 μ W. A piezoelectric cantilever was miniaturized and placed in the shoe by Fan *et al.*¹⁴ to produce 0.35mW at a walking speed of 8km/h. Gao *et al.*¹⁵ utilized a slider-crank mechanism to transform the rotary motion of a knee joint to a linear motion and generate 1.6mW for a total weight of just 307g. Michael *et al.*¹⁶ designed a harvester based on the impact of a moving mass on piezoelectric bending structures.

Despite the diversity of existing energy harvesting structures, the output power which has been generated remains low to achieve truly self-powered wearable devices. The underlying difficulty of achieving a higher output power lies in both the low-frequency and irregularity of human motion. Therefore, the transformation of low-frequency human motion into an high-frequency energy harvesting motion has attracted the interest of many researchers¹⁷⁻¹⁹. Zhang *et al.*²⁰ fabricated a rotational electromagnetic energy harvester with a twisting driving structure and a ratchet-clutch structure, where the maximum speed of the ratchet can be as high as 3700rpm. Fan *et al.*²¹ proposed a rope-driven rotor that can undertake high-speed rotation during ultra-low frequency

excitation. Wang *et al.*²² developed a magnetic-spring harvester to transform the low-frequency swing of the lower-limb to high-frequency oscillation of magnets. Cai *et al.*²³ designed an electromagnetic generator with a magnetic frequency-up converter and generated an average power of 1.74mW.

It is clear that the range of frequency up-conversion structures mentioned above enable and improvement in the performance of human motion energy harvesters. However, the total weight of the energy harvesters for human motion is often one of most significant constraints in the real-world applications. A compact structure of magnetic field modulation²⁴ can be employed to achieve a frequency up-conversion function, without having a strong influence of the human effort required for walking. Moreover, it can eliminate any potential collision between oscillating magnets and stator magnets at higher accelerations^{6,22}. Finally, the convenience and comfort of the harvesting worn during walking and running is an additional important factor. A simple and integrated structure design, such as stacked layers, is therefore required to improve the reliability and decrease the influence of supplementary components on human motion. As a result, this paper proposes a new stacked electromagnetic harvester with frequency up-conversion to enhance the energy harvesting performance from limb swing, where the device architecture is shown in [Fig. 1](#).

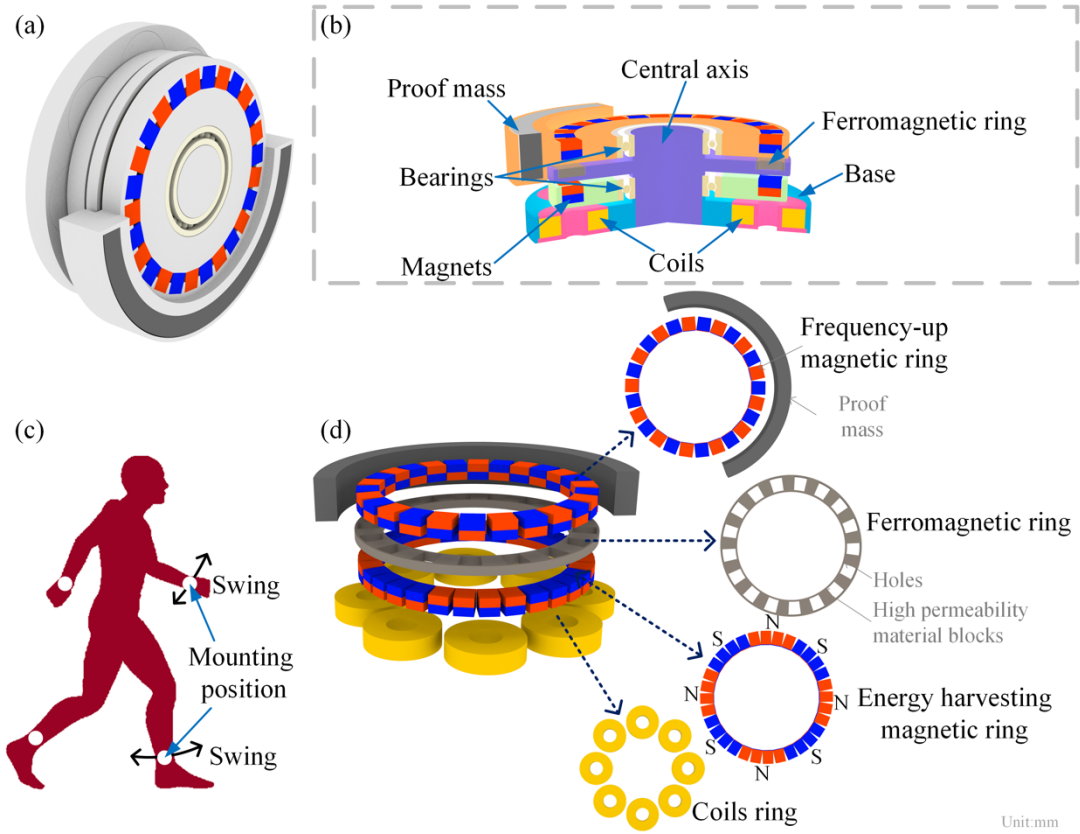


FIG. 1. Design and mounting position of the harvester. (a) Structure of the harvester. (b) Sectional view. (c) Mounting position on human body. (d) Critical parts.

Fig. 1(a)-(d) demonstrate the structure of the harvester and its mounting position on the human body. The critical parts of the harvester are four rings which include a ferromagnetic ring, harvesting magnetic ring, coil rings and frequency up-conversion magnetic ring, as shown in Fig. 1(d). The working principle of the harvester is as follows: when the harvester is attached to the upper-limb or lower-limb, as shown in Fig. 1(b,c), the proof mass will rotate around the central axis during excitation by human motion. The frequency up-conversion magnetic ring, as well as its magnetic field, will rotate and follow the proof mass. The harmonic order of rotating magnetic field will change after it passes the ferromagnetic ring²⁵, while the energy harvesting magnetic ring will rotate at a higher speed under the driving magnetic force. As a result, the magnetic flux inside the coils will change and generate an inductive voltage.

The number and layout of magnets must be carefully designed in order to achieve magnetic modulation, as shown in Fig. 1(d). The transmission ratio G_r depends on the pole pairs of the two magnetic rings:

$$G_r = \frac{P_f}{P_e} \quad (2)$$

where P_f is the number of pole pairs of the frequency up-conversion magnetic ring, and P_e is the number of pole pairs of energy harvesting magnetic ring.

As shown in Fig. 1(d), frequency-up magnetic ring is formed by 26 magnets with size of $5\text{mm} \times 5\text{mm} \times 4\text{mm}$, and the orientation of adjacent magnets is in an opposite direction to form 13 pole pairs. The energy harvesting magnetic ring consists of 32 magnets with size of $4\text{mm} \times 5\text{mm} \times 4\text{mm}$, where four magnets are in the same orientation and can be seen as one magnetic pole. Therefore, the pole pairs of energy harvesting magnetic ring is 4, making the transmission ratio of the prototype 13:4. All magnets are made using sintered NdFeB, N50, and the ferromagnetic ring is manufactured by high permeability material (typically, silicon steel) with holes arranged uniformly in the circumferential direction. The holes and high permeability material blocks are in same size and alternately arranged, the number of holes equals the sum of pole pairs of two magnetic rings. The coils ring has eight coils connected in series and each coil has 500 turns and the total resistance of the coil ring is 140Ω .

Two magnetic rings, the harvesting magnetic rig and frequency up-conversion magnetic ring, are employed in the harvester, as shown in Fig. 1(d). The magnetic fields that they generate is a key factor for frequency up-conversion and energy harvesting. A theoretical model aiming to depict the magnetic fields is constructed based on the method proposed by Zhang *et al*²⁶, where the magnetic

field strength and the magnetic flux density produced by cubic magnet ($2a \times 2b \times 2c$) at a specific point $P(x_0, y_0, z_0)$ can be calculated by Eqs. (3)-(4).

$$H = \frac{J}{4\pi\mu_0} \sum_{k=0}^1 \sum_{i=0}^1 \sum_{j=0}^1 (-1)^{(i+j+k)} \varepsilon(U, V, W) \quad (3)$$

$$B = \mu_0 H = \frac{J}{4\pi} \sum_{k=0}^1 \sum_{i=0}^1 \sum_{j=0}^1 (-1)^{(i+j+k)} \varepsilon(U, V, W) \quad (4)$$

Therefore, the magnetic flux density in the z -direction of point $P(x_0, y_0, z_0)$ can be indicated as:

$$B_z(x_0, y_0, z_0) = \sum_{j=1}^{32} B_{jz}(x_0, y_0, z_0) \quad (5)$$

Where B_{jz} represent the z -direction magnetic flux density of j th magnet in the point $P(x_0, y_0, z_0)$.

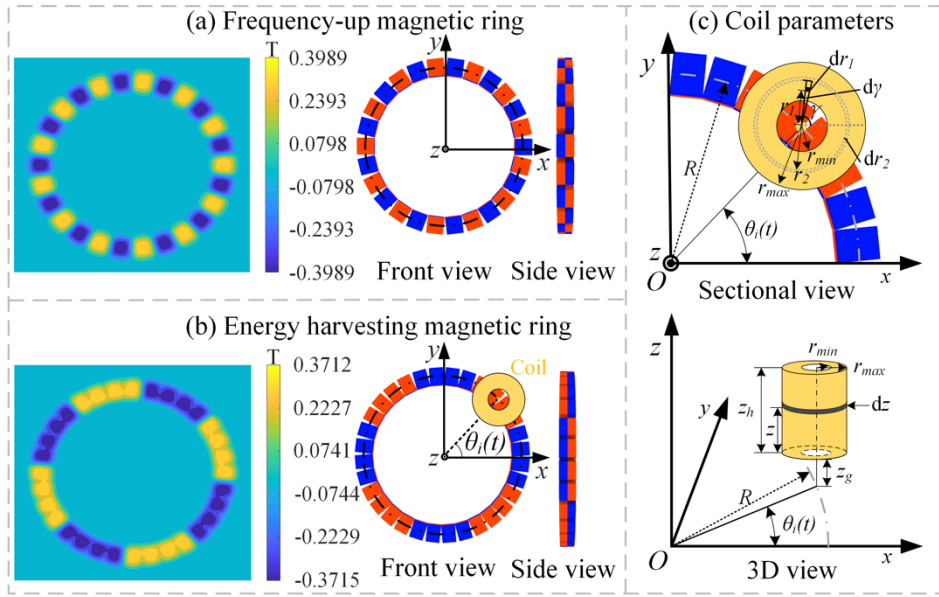


FIG. 2. Magnetic flux density in z -direction. (a) Magnetic flux density of frequency-up magnetic ring. (b) Magnetic flux density of energy harvesting magnetic ring. (c) Coils parameters.

Fig. 2 shows magnetic flux density of the two magnetic rings (harvesting ring and up-conversion ring) with a 1mm air gap between the observation plane and permanent magnets. The magnetic flux density of the frequency up-conversion magnetic ring can reach up to 0.399T with 26 magnetic poles, which is generated by 26 alternately arranged magnets. The magnetic flux density, as well as the front view and side view of energy harvesting magnetic ring, is shown in Fig. 2(b) with a coil shown.

The magnetic distribution of energy harvesting magnetic ring with 32 magnets shows 8 magnetic poles, in which each magnetic pole is composed of 4 magnets. The maximum magnetic flux density of energy harvesting ring is 0.371T, which is slightly lower than that of frequency up-conversion magnetic ring.

Based on the theoretical model of magnetic fields, the performance of harvester can be predicted according to Faraday's law. The magnetic flux inside the coil can be obtained by integrating the magnetic flux density throughout the coils. Assuming that the number of coils turns is uniformly distributed in the radial direction and along the z -direction, the magnetic flux of i th coils can be expressed as:

$$\phi_i(t) = \int_0^{z_h} \int_{r_{\min}}^{r_{\max}} \int_0^{r_2} \int_0^{2\pi} B_z(R \sin(\theta_i(t)) + r_1 \cos \gamma, R \cos(\theta_i(t)) + r_1 \sin \gamma, z + z_g) \frac{n}{z_h} \frac{1}{r_{\max} - r_{\min}} r_1 d\gamma dr_1 dz dr_2 \quad (6)$$

where Z_h is the height of i th coils in the z -direction, R_{\max} and R_{\min} are the outside and inside diameter of coils respectively, $\theta_i(t)$ indicates the coils' position. R is the central diameter of magnetic ring. z_g is the air gap between coils and magnets. Those parameters are indicated by Fig. 2 (c).

The total inductive voltage of harvester can be expressed as:

$$U = - \sum_{i=1}^8 \frac{d\phi_i(t)}{dt} \quad (7)$$

A prototype is fabricated based on these discussions. Firstly, the harvester is mounted on a motor to verify its frequency up-conversion functionality. The frequency-up magnetic ring rotates with the shaft of the motor, while the coil ring, central shaft and ferromagnetic ring are held still by a plastic plate, as shown in the Fig. 3(a). The inductive voltage is determined by an oscilloscope (DSO-X 3012A) and a resistance of 140Ω is connected to the coils ring to demonstrate its energy harvesting performance.

Fig. 3(b). shows the sinewave-like voltage signal generated inside the coil ring. The rotation speed of energy harvesting magnetic ring can be obtained by the frequency of generated voltage signal, where the relation can be denoted as:

$$n_e = \frac{60f}{p_e} \quad (8)$$

Where n_e (unit: rpm) represents the rotation speed of energy harvesting magnetic ring, f represents the frequency of generate voltage, and P_e is the number of pole pairs of energy harvesting magnetic ring.

The inductive open circuit voltage under an input rotation speed of 152rpm, 248rpm and 344rpm are chosen to verify the theoretical prediction of the model. The results are shown in the Fig. 3(b), which shows that the theoretical model precisely predicts the amplitude and phase of experimental voltage. The average voltage from the experiments are 4.12V, 6.71V and 9.29V respectively, the corresponding average voltages are 4.11V, 6.71V and 9.31V in the theoretical prediction. The agreement with experiment and model results is excellent, with a maximum error of less than 0.25%.

The rotation speed ratio of energy harvesting magnetic ring and frequency up-conversion magnetic ring is 13:4. The maximum ration speed error of energy harvesting magnetic ring is 1rpm, as denoted by Fig.3 (c), and the maximum average power generated across the load resistance is 0.156W.

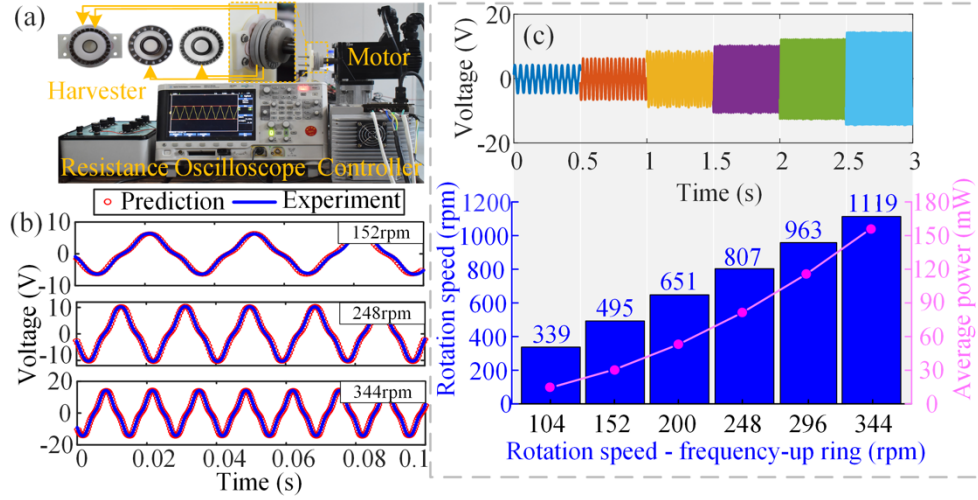


FIG. 3. Experimental set-up and results. (a) harvester mounted on the motor. (b) Experimental open circuit voltage and theoretical prediction. (c) Rotation speed of energy harvesting magnetic ring and generated average power.

In addition to experiments on a motor, the performance of the harvester is also evaluated under human motion. The experimental set up is similar with previous experiments and the harvester is attached to the upper and lower-limb of human body by nylon tape, and connected to a resistance of 140Ω , as shown in Fig.4 (a). An acceleration sensor (MEMSIC, CXL04GP3) is also placed near the harvester to measure the human motion excitation in the swing direction; perpendicular to the upper or lower-limb.

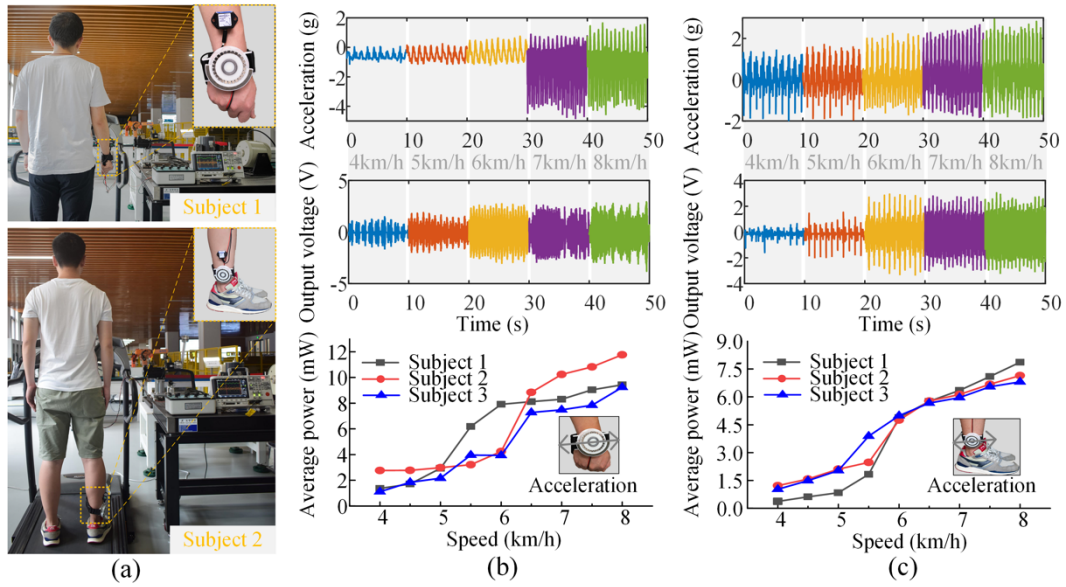


FIG. 4. Experiments under human motion. (a) Experimental set up. Captured excitation, voltage and calculated average power when attached to upper-limb (b) and lower-limb (c).

As indicated in [Fig.4 \(a\)](#), three subjects (Subject 1: male, 173cm/73kg. Subject 2: male, 170cm/68kg. Subject 3: female, 169cm/66kg) walk and run on a treadmill at speeds ranging from 4-8km/h (4-6km/h walking, 6.5-8km/h running). [Fig.4 \(b\)-\(c\)](#) shows the acceleration and voltage in a single measurement of ten seconds, where the mean value of average output power for three measurements are also presented. An acceleration surge is observed in the process of switching from walking to running when attached to the upper-limb, with the maximum value of $\sim 5g$ ($g=9.81\text{m/s}^2$). However, the generated voltage does not change significantly and one possible reason is that the excessive acceleration is beyond the torque transmission range of the harvester, therefore the energy harvesting magnetic ring cannot follow the rotation of the frequency up-conversion magnetic ring.

At a normal walking speed of approximately 5km/h, the maximum acceleration and voltage of the harvester attached to upper-limb can reach up to 1.1g and 2V, where the corresponding average power is around 2.7mW. When attached to the lower-limb, the acceleration, voltage and power become 1.9g, 2V and 1.6mW respectively. In the case of running at a speed of 7 km/h, the average output power for subject 1, 2 and 3 is 8.3mW, 10.2mW and 7.5 mW on the upper-limb, and 6.3mW, 6.1mW and 6.0mW for the lower-limb. Overall, the harvester tends to generate more energy when attached to upper-limb than lower-limb since..... The maximum power is 9.4mW, 11.8mW and 9.2mW for subject 1, 2 and 3 when attached to upper-limb ([Fig 4b](#)) , and 7.9mW, 7.1mW and 6.8mW for lower-limb ([Fig 4b](#)). Overall, the maximum average power generated under human motion is 11.8mW with a total harvester weight of 190.7g, corresponding to a power density is $61.9\mu\text{W}\cdot\text{g}^{-1}$. The excellent performance of harvester makes it possible to powering low-power device by harvesting energy from human motions (see [Supplementary Video 1-3](#)).

In summary, an electromagnetic energy harvester is designed and fabricated with a novel stacked ring geometry to extract energy from limb swing to realize a frequency up-conversion function. The magnetic field of the magnetic ring and inductive voltage are calculated using a theoretical model. The frequency up-conversion function is assessed by constant rotating experiments, where the average power reaches 0.156W under input rotation speed of 344rpm. Theoretical predictions show excellent agreement with experimental results. The experiments under human motion indicates the maximum average power generated is 11.8mW with a total device weight of 190.7g, corresponding to a power density of $61.9\mu\text{W}\cdot\text{g}^{-1}$. The excellent performance in terms of high power density provides potential application in self-powered wearable energy harvesting devices and systems..

Support from National Natural Science Foundation of China (Grant No. 51575426, 51811530321) and Royal Society (Grant No. IEC\NSFC\170589).

- ¹ F. Qian, T.-B. Xu, and L. Zuo, [Smart Mater. Struct.](#) **28** (7), 075018 (2019).
- ² F. Qian, T.-B. Xu, and L. Zuo, [Energy Convers Manage.](#) **171**, 1352 (2018).
- ³ K. Tao, H. Yi, Y. Yang, H. Chang et al. [Nano Energy.](#) **67**, 104197 (2020).
- ⁴ S. Wang, Y. Xie, S. Niu, L. Lin et al. [Adv. Mater.](#) **26** (18), 2818 (2014).
- ⁵ K. Fan, M. Cai, H. Liu, and Y. Zhang. [Energy.](#) **169**, 356 (2019).
- ⁶ K. Fan, Y. Zhang, H. Liu, M. Cai et al. [Renewable Energy.](#) **138**, 292 (2019).
- ⁷ Y. Yuan, M. Liu, W.-C. Tai, and L. Zuo, [J. Mech. Des.](#) **140** (8), 085001 (2018).
- ⁸ H. Liu, C. Hou, J. Lin, Y. Li et al. [Appl. Phys. Lett.](#) **113** (20), 203901 (2018).
- ⁹ L. Xie and M. Cai, [J. Mech. Des.](#) **137** (5), 054503 (2015).
- ¹⁰ J. M. Donelan, Q. Li, V. Naing, J. Hoffer et al. [Science.](#) **319** (5864), 807 (2008).
- ¹¹ M. Evans, L. Tang, K. Tao, and K. Aw. [Sens. Actuators, A.](#) **285**, 613 (2019).
- ¹² L. C. Rome, L. Flynn, E. M. Goldman, and T. D. Yoo. [Science.](#) **309** (5741), 1725 (2005).
- ¹³ M. Halim, R. Rantz, Q. Zhang, L. Gu et al. [Appl. Energy.](#) **217**, 66 (2018).
- ¹⁴ K. Fan, Z. Liu, H. Liu, L. Wang et al. [Appl. Phys. Lett.](#) **110** (14), 143902 (2017).
- ¹⁵ F. Gao, G. Liu, B. L.-H. Chung, H. H.-T. Chan et al., [Appl. Phys. Lett.](#) **115** (3), 033901 (2019).
- ¹⁶ M. Renaud, P. Fiorini, R. van Schaijk, and C. Van Hoof. [Smart Mater. Struct.](#) **18** (3), 035001 (2009).
- ¹⁷ S. Wei, H. Hu, and S. He. [Smart Mater. Struct.](#) **22** (10), 105020 (2013).
- ¹⁸ K. Fan, M. Cai, F. Wang, L. Tang et al. [Energy Convers Manage.](#) **198**, 111820 (2019).

- ¹⁹ P. Pillatsch, E. M. Yeatman, and A. S. Holmes. [Sens. Actuators, A.](#) **206**, 178 (2014).
- ²⁰ Y. Zhang, A. Luo, Y. Wang, X. Dai et al. [Appl. Phys. Lett.](#) **116** (5), 053902 (2020).
- ²¹ K. Fan, H. Qu, Y. Wu, T. Wen et al. [Renewable Energy](#) **156** (2020).
- ²² W. Wang, J. Cao, N. Zhang, J. Lin et al. [Energy Convers Manage.](#) **132**, 189 (2017).
- ²³ M. Cai, J. Wang, and W.-H. Liao. [Appl. Energy](#) **263**, 114682 (2020).
- ²⁴ S. Mezani, K. Atallah, and D. Howe, J. [Appl. Phys.](#) **99** (8), 08R303 (2006).
- ²⁵ K. Atallah and D. Howe. [IEEE Trans. Magn.](#) **37** (4), 2844 (2001).
- ²⁶ Y. Zhang, J. Cao, W.-H. Liao, L. Zhao et al. [Smart Mater. Struct.](#) **27** (9), 095019 (2018).